Morphometric analysis of urban fluvial terraces using UAV LiDAR: A case study from the Santa Catarina River, Mexico

Mariana Pérez-Martínez[1], Fabiola D. Yépez-Rincón[1*], Luis E. Arista-Cázares[1], Yadira Z. Antonio-Durán[1], Kevin D. Rodríguez-González[1], Héctor de León-Gómez, Adrián L. Ferriño-Fierro[1] and Víctor H. Guerra-Cobián[1].

[1]Faculty of Civil Engineering, Universidad Autónoma de Nuevo León, San Nicolás de los Garza, Nuevo León, México
*fabiola.yepezrn@uanl.edu.mx

Keywords: urban river, point clouds, fluvial geomorphology, terrace mapping, anthropogenic impact.

ABSTRACT:

This study analyzes the geomorphological evolution of fluvial terraces along the urban section of the Santa Catarina River (Nuevo León, México) by integrating high-resolution UAV-based LiDAR and photogrammetry. Six areas corresponding to previously reported cross-sections (A-F) were surveyed, analyzed and temporarily compared through digital elevation models, morphometric indices, and RGB orthomosaics. The results highlight significant anthropogenic impacts, including solid waste accumulation, hydraulic lining, and bridge construction, which have altered the morphology and visibility of several terraces. In contrast, area from the cross-section F-F', less disturbed by human intervention, enabled detailed topographic and lithological characterization. Four terraces (T0-T3) were identified reflecting distinct depositional phases and energy regimes. The influence of recent tropical cyclones (Fernando, Hanna, and Alberto) was also visualized, revealing vegetation loss and terrace modification. UAV-LiDAR technology proved effective for high-precision mapping of urban fluvial systems and offers valuable tools for hydromorphological monitoring.

1.Introduction

Fluvial terraces are low-relief, step-like landforms that develop alongside river valleys, typically formed through alternating periods of lateral erosion and vertical incision. These landforms result from the deposition of alluvial sediments during stable hydrological phases, followed by incision events that isolate former floodplain surfaces above the active riverbed. As such, fluvial terraces preserve important records of sedimentological, hydrological, and geomorphic history, reflecting changes in base level, tectonic uplift, climate variability, and land use dynamics (Pederson et al., 2006).

In regions affected by tropical cyclones, these events can significantly alter sediment transport and river morphology, thereby influencing the formation and distribution of fluvial terraces. Terraces often originate from rapid sedimentation associated with extreme precipitation events, where floods mobilize large volumes of sediment (Sánchez-Núñez et al., 2014). Consequently, terraces serve as a continental archive of both climatic and tectonic changes (Tlapáková et al., 2021; Delchiaro et al., 2024), and their morphology can be sensitive to anthropogenic disturbances as well.

The Santa Catarina River is one of the three urban rivers that flow through the Monterrey Metropolitan Area (MMA, México) (Nagel-Vega, 2023). Since the last documented fluvial terrace analysis (Martínez-Quiroga, 2018), the river has been affected by at least three tropical cyclone events. These events have likely contributed to significant geomorphic modifications along the river course, including the redistribution or partial degradation of terrace structures.

The MMA exhibits significant structural and environmental deficiencies that increase its vulnerability to extreme hydrometeorological events. Key contributing factors include unregulated land-use changes, limited availability of geospatial information for risk management, and disorganized urban expansion. Institutional responses following catastrophic events have revealed the lack of monitoring systems and integrated databases, which severely limits the capacity for effective planning, mitigation, and prevention (Yépez et al., 2013).

In this context, the use of Unmanned Aerial Vehicle (UAV) LiDAR sensors has proven highly effective for the evaluation, monitoring, and mapping of fluvial terraces (Li et al., 2019; Niculiță et al., 2020; Iacobucci et al., 2022). UAV-LiDAR systems offer high-resolution topographic data, efficient deployment in challenging terrain, and the ability to detect fine-scale surface variation even under moderate vegetation cover. Compared to traditional surveying methods such as Global Navigation Satellite System (GNSS) or photogrammetry alone, UAV-LiDAR enables greater vertical accuracy and bare-earth modeling, making it especially suitable for fluvial geomorphology and morphometric analysis (Iacobucci et al., 2022).

This study aims to assess changes in the morphology and spatial distribution of fluvial terraces along the urban reach of the Santa Catarina River by comparing a terrace inventory from 2018 with new high-resolution LiDAR data collected in 2025 using a UAV platform. The analysis integrates digital elevation models (DEMs), morphometric indices, and GIS-based spatial analysis to evaluate terrace preservation, detect potential erosional or anthropogenic alterations, and better understand fluvial dynamics in a heavily urbanized environment.

1.1 Study Site

The Santa Catarina River rises at about 2200 meters above sea level (m a.s.l.) in the Sierra de San José de los Nuncios, in the Center-West of the state of Nuevo León, which runs through a structurally complex area, dominated by Cretaceous sedimentary rocks, associated with the orogeny of the Sierra Madre Oriental.

The river flows from west to east towards the MMA, crossing the Los Muertos anticline at 680 m a.s.l. From here, the river crosses six municipalities of the MMA, these being: Santa Catarina, San Pedro Garza García, Monterrey, Guadalupe, Juárez, and Cadereyta, respectively, where it flows into the San Juan River, which feeds the Rio Grande at approximately 400 m a.s.l. Figure 1 reflects the geographical context of the study area.

This contribution has been peer-reviewed. The double-blind peer-review was conducted on the basis of the full paper.
https://doi.org/10.5194/isprs-annals-X-3-W3-2025-77-2026 | © Author(s) 2026. CC BY 4.0 License.

The area is characterized by incised fluvial terraces, intermittent flow, and braided segments. These terraces are mainly composed of unconsolidated Quaternary alluvial deposits such as gravel, sand, and silt. These materials reflect episodic sedimentation and incision events, controlled by regional tectonics and climatic variations (Martínez-Quiroga, 2021). The alluvial deposits overlie a lithological basement formed by the Upper Cretaceous Méndez Formation, which consists of light greenish-brown and gray laminated shales and marls with a high degree of fracturing (Michalzik, 1988). Overall, the terrace system represents a geomorphological archive of high relevance for the analysis of fluvial processes and the evolution of the landscape in an urban environment in constant transformation.

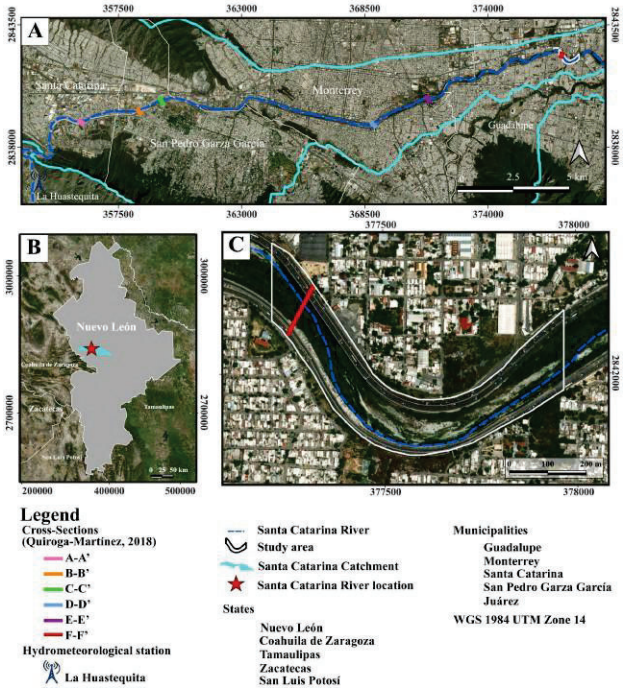

Figure 1. Location map. (A) Urban reach of the Santa Catarina River in MMA, (B) Nuevo León, México. (C) F-F' cross section area.

2. Methodology

2.1 UAV Platform and Data Acquisition

Data acquisition was conducted between May and June 2025 using a DJI Matrice 350 RTK (Real-Time Kinematic) (Table 1), equipped with a Zenmuse L2 high-resolution LiDAR sensor (Table 2) (Figure 2). This sensor integrates a laser scanner, a high-precision inertial measurement unit (IMU), and an RGB camera, enabling the simultaneous acquisition of dense 3D point clouds and high-resolution orthophotos. Under optimal GNSS conditions, the system achieved a horizontal accuracy of approximately 5 cm, a vertical accuracy of 4 cm, and a range RMSE of 2 cm. The RGB camera captured imagery with an average ground sampling distance (GSD) of 3 cm.

DJI MATRICE 350 RTK			
Max. Flight Time	**Max. Transmission Distance**	**Hovering Accuracy (with moderate or no wind)**	**RTK Accuracy**
Approx. 55 min (under no-wind conditions)	8 km (with unobstructed, free of interference)	±0.1 m (horizontal) ±0.1 m (vertical), with RTK positioning	1 cm + 1 ppm (horizontal) 1.5 cm + 1 ppm (vertical)

Table 1. Key technical specifications of the DJI Matrice 350 RTK used in this study.

A total of six UAV flights were conducted, one for each of the six mapped terrace segments. Flights were executed at an average altitude of 100 m above ground level (AGL), with a forward overlap of 40% and a side overlap of 70%, ensuring sufficient point density and full surface coverage. The average flight speed was 7.64 m/s, with each mission lasting approximately 14 minutes, allowing for single-battery operation per flight. All spatial data were projected to the WGS84/UTM zone 14N coordinate system (EPSG: 32614).

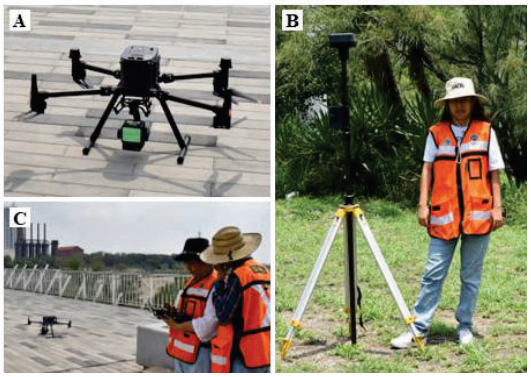

Figure 2. Equipment used in the field: (A) DJI Matrice 350 RTK with the Zenmuse L2 sensor, (B) installation of the RTK positioning system, and (C) verification of the equipment with the remote control for the start of the flight.

Real-time corrections were enabled through a GNSS base station connected via NTRIP protocol, which ensured precise georeferencing through RTK positioning. During the flights, the Zenmuse L2 LiDAR sensor operated in repetitive scanning mode with a field of view (FOV) of 70° × 3° and a pulse repetition frequency of 240 kHz, producing a high-density scan pattern (DJI, 2023). The resulting ground beam footprint was approximately 117 mm × 39 mm. Effective LiDAR data collection per flight lasted 11 minutes and 24 seconds, while the position and orientation system (POS) remained active for 13 minutes and 6 seconds, maintaining an RTK-fixed status for 99.49% of the flight duration.

ZENMUSE L2 SENSOR			
Pulse frequency (kHz)	**Sampling rate (Hz)**	**Horizontal FOV (°)**	**Max returns**
240	200	±70	5

Table 2. Key technical specifications of the Zenmuse L2 LiDAR sensor used in this study.

2.2 Data Processing

The acquired LiDAR and RGB data were processed using DJI Terra software version 4.5.0, following a multi-stage workflow designed to optimize point cloud quality and accuracy. The processing steps included automated routines for initial point cloud alignment, georeferencing using RTK metadata, and noise filtering, followed by smoothing and precision adjustments to enhance surface continuity and model fidelity.

After processing, the data were exported in standardized formats to facilitate subsequent analysis. These included PNTS and LAS formats for point cloud data; B3DM, PLY, and OBJ for 3D modeling applications; and GeoTIFF for generating high-resolution DEMs. This multi-format output ensured interoperability with diverse geospatial and remote sensing platforms, including GIS and 3D modeling environments.

This contribution has been peer-reviewed. The double-blind peer-review was conducted on the basis of the full paper.
https://doi.org/10.5194/isprs-annals-X-3-W3-2025-77-2026 | © Author(s) 2026. CC BY 4.0 License.

2.3 Morphometric Analysis

To analyze the geomorphological properties of the fluvial terraces, four morphometric indices were derived from a high-resolution DEM with a spatial resolution of 0.5 m. The selected indices were: slope, topographic position index (TPI), terrain ruggedness index (TRI), and elevation standard deviation (ESD). These metrics quantify surface inclination, relative topographic position, terrain complexity, and local elevation variability, respectively. The selection of these indices was based on their proven effectiveness in identifying flat surfaces, terrace scarps, erosion features, and microtopographic irregularities in fluvial environments.

2.4 Orthomosaic Analysis

An RGB orthomosaic was generated from the aerial imagery captured during the same UAV flights using the integrated photogrammetric sensor of the Zenmuse L2. The images were processed in DJI Terra, where sequential steps of image alignment, georeferencing, and mosaic stitching were performed. The resulting orthomosaic had a spatial resolution of approximately 3 cm per pixel, enabling detailed visualization of surface features. This orthomosaic served as a valuable reference for the visual interpretation of land surface characteristics, including vegetation cover, terrace boundaries, erosional features, and anthropogenic modifications. In addition, it supported the validation of LiDAR-derived terrain features and was used to digitize terrace margins and establish control points for subsequent morphometric and spatial analyses.

2.5 Elevation Analysis by Point Clouds

The elevation analysis was conducted using the classified LiDAR point clouds obtained from the Zenmuse L2 sensor. These point clouds were georeferenced in real time using RTK corrections, ensuring centimeter-level positional accuracy. Following the initial preprocessing, ground points were classified and filtered to exclude vegetation and non-ground returns, allowing the generation of a bare-earth surface.

From the classified ground points, a DEM was interpolated with a spatial resolution of 0.5 m. This DEM served as the primary input for deriving topographic variables and performing morphometric analyses, as well as for comparing elevation profiles across the mapped fluvial terraces.

2.6 Identification of Socio Environmental Factors

A systematic identification of socio-environmental factors was conducted using high-resolution UAV orthomosaics. A visual interpretation key was followed to ensure consistency during the identification, based on tone, texture, shape, pattern, and spatial association (Table 3), additional to ground level observations. Each orthomosaic was carefully photo interpreted allowing to georeference areas directly in QGIS, where they were saved in a geodatabase.

2.7 Geomorphological and Lithological Analysis of the Fluvial Terraces

The identification and characterization of the fluvial terraces were carried out through the interpretation of DEMs, orthomosaics, point clouds, and contour lines obtained from drone-based photogrammetric and LiDAR surveys. These geospatial products enabled a high-resolution topographic delineation and precise visual interpretation of the different terrace levels. Spatial analysis was conducted using ArcGIS Pro software, where the geomorphological boundaries of the units were defined and compared with those proposed in previous studies. Additionally, a detailed comparison of topographic profiles was performed using AutoCAD software.

Category	Visual indicators	Interpretation criteria
Solid waste accumulation	Scattered, irregular patches of multicolored debris, near the river	Heterogeneous textures with no vegetation
Construction debris	Angular objects near construction areas	Coarse, near roads or exposed ground
Housing within the riverbed	Small structures inside or adjacent to the active channel	Rectangular rooftops within the floodplain and terrace levels
Civil works	Retaining walls or columns under construction	Regular geometric forms, adjacent to modified river sections
Wastewater discharge	Dark stains or channels emerging from the hydraulic lining	Linearly shaped discolorations near infrastructure or drainage
Artistic sculptures	Isolated objects with distinctive shapes	Unusual, near the river channel,
Urban parks	Green patches with regular paths, benches, or recreational structures	Vegetated zones with infrastructure indicating planned public space
Hydraulic lining	Continuous, straight-edged linings along the river channel	Uniform textures and tones indicating concrete channelization
Footbridges	Narrow linear structures with pedestrian pathways and shadows	Aligned across the channel; thinner and narrower than vehicle bridges
Vehicular bridges	Wide linear structures connected to major roadways	Broader with lane markings, shadows from guardrails or vehicles

Table 3. Visual interpretation key for socio-environmental factors.

3. Results

3.1 Photogrammetry and Point Cloud Post-processing

Photogrammetric post-processing was performed using DJI Terra software, which generated both DEMs and orthomosaics from the UAV-acquired imagery. Each terrace area required approximately 1 hour and 27 minutes of processing time (Tabla 4).

Terrace área	Images	Mapping Coverage (km^2)	GSD (cm/px)	PCAD (points/m^2)
A	252	0.32	3.00	288
B	311	0.41	3.11	313
C	351	0.42	3.14	585
D	307	0.35	2.91	272
E	304	0.41	2.95	318
F	405	0.31	3.08	149

Table 4. Summary of flight and point cloud characteristics for each terrace site. GSD: Ground Sample Distances; PCAD: Point Cloud Average Density.

To enhance visualization and interpretability, the RGB imagery captured during the flights was fused with the LiDAR point cloud, assigning real-world color values to each 3D point. This fusion improved the identification of surface features and supported further spatial analysis.

The resulting DEM achieved high cartographic resolution, supporting accurate mapping at a 1:500 scale, and was accompanied by a textured 3D mesh and a true-color orthomosaic with a spatial resolution of 3.08 cm/pixel. Point cloud density was processed at 100% resolution, with an effective detection range of 0.5 to 300 m.

As shown in Figure 3A, a dense point cloud was generated using Structure-from-Motion (SfM) techniques applied to UAV imagery over the urban river corridor. The 3D reconstruction captures both natural features (e.g., riverbed, vegetation) and anthropogenic structures (e.g., roads, bridges).

Figure 3B presents the same point cloud classified by elevation, visualized using a continuous color ramp from blue (low elevation) to red (high elevation), ranging approximately from 441 to 492 m above sea level. This elevation gradient emphasizes vertical variations in the terrain and allows the identification of key geomorphic features, including floodplains, terrace edges, and channel incisions.

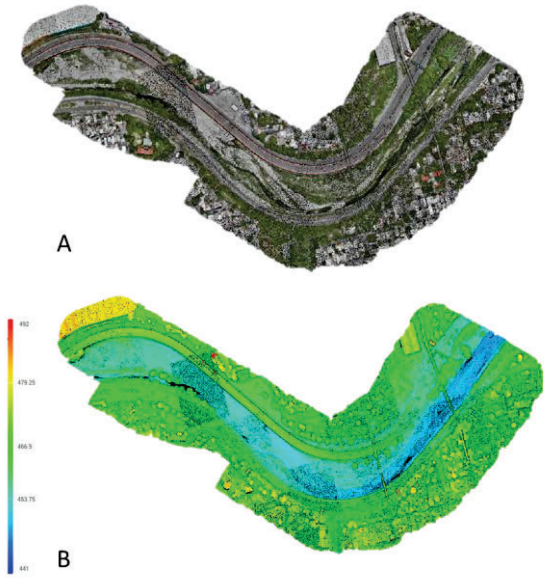

Figure 3. Point clouds: (A) RGB, and (B) height.

Figure 4A shows the LiDAR return intensity, with a spectral gradient from blue (low intensity) to red (high intensity). These values reflect differences in surface reflectance, which are influenced by material type, surface roughness, and orientation, helping to distinguish vegetation, built-up areas, and bare ground.

In Figure 4B, the number of returns per pulse (ranging from 1 to 5) is shown. Higher return counts indicate complex vertical vegetation structures, while single returns correspond to solid or impervious surfaces, providing valuable insights into the vertical stratification of the riverine environment.

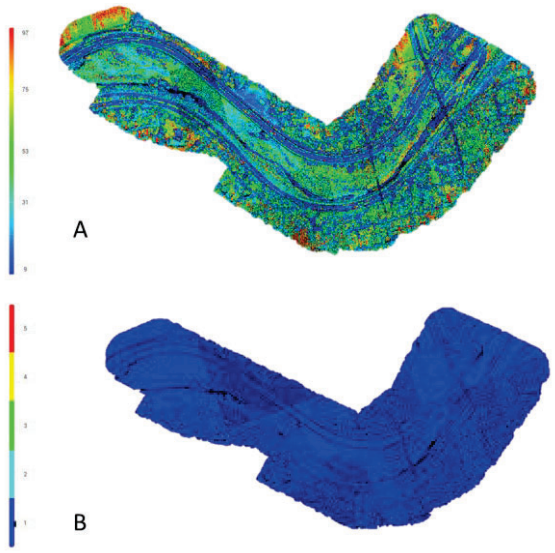

Figure 4. Point clouds: (A) intensity, and (B) return number.

3.2 Influence of Socio-environmental Factors on the Characterization of Fluvial Terraces

The socio-environmental factors that have contributed to the modification of the fluvial terraces include the accumulation of solid waste, bridges, and hydraulic linings, among others. Additionally, some of these factors, such as the rapid construction of bridges, obstruct the aerial view of the riverbed, posing a significant challenge for terrace identification and characterization using UAVs.

Figure 5 shows a compilation of orthomosaics processed in this study, corresponding to the terrace areas A–F previously delineated by Martínez-Quiroga (2018). Terraces A–A', B–B', C–C', D–D', and E–E' have undergone notable anthropogenic alterations, including waste accumulation, landscaping, metro line construction, and channel lining. Moreover, terraces B–B', C–C', and E–E' are now partially covered in aerial view by pedestrian and vehicular bridges.

In contrast, in section F–F' are partially covered by road infrastructure, this segment preserves a more continuous geomorphic profile compared to the other five sections, making it suitable for detailed analysis. For this reason, it was selected for detailed geomorphic and point cloud-based analysis and comparison in this study.

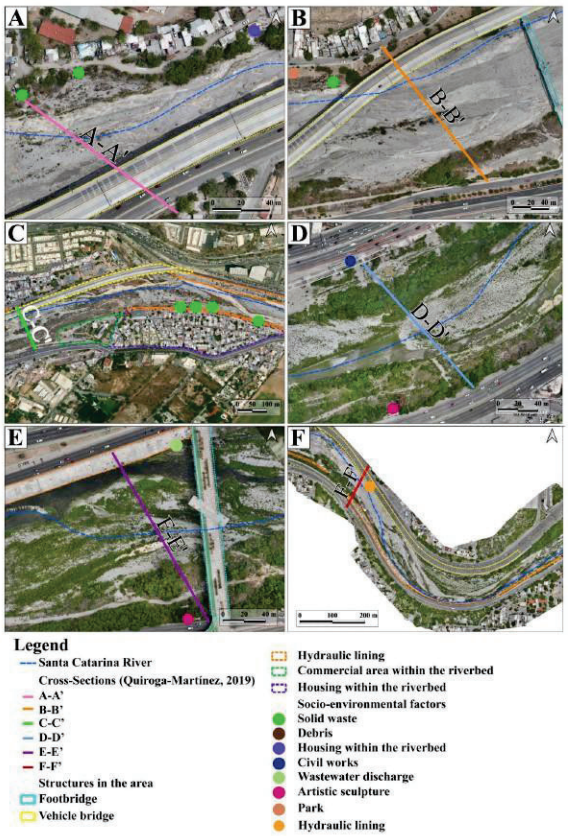

Figure 5. Orthomosaics of terrace areas. Orthomosaics of terrace sections A–F, as delineated by Martínez-Quiroga (2018). Sections A–A', B–B', C–C', D–D', and E–E' show anthropogenic modifications, including solid waste deposition, infrastructure development, and hydraulic channel linings. B–B', C–C', and E–E' are influenced by pedestrian or vehicular bridges. Section F–F' presents minimal disturbance and retains a continuous geomorphic profile, making it suitable for detailed analysis.

This contribution has been peer-reviewed. The double-blind peer-review was conducted on the basis of the full paper.
https://doi.org/10.5194/isprs-annals-X-3-W3-2025-77-2026 | © Author(s) 2026. CC BY 4.0 License.

3.3 Morphometric Analysis

The slope (Figure 6A) was computed in ArcGIS Pro using the Spatial Analyst toolbox. This index represents the degree of surface inclination at each raster cell, expressed in degrees. In the study area, slope values ranged from 0° to 78.13°, identifying both flat terrace surfaces and steep scarp edges.

The TPI (Figure 6B) measures the relative elevation of a given cell concerning its surrounding neighborhood (Reu et al., 2013). This index was calculated using the Geospatial Data Abstraction Library (GDAL) within QGIS. Values ranged from 1.42 m to 1.36 m, with negative values (< 0) corresponding to deeply incised channels, that is, sediment deposition zones, and positive values (> 1) indicating prominent elevations such as terrace edges, ridges, or escarpments, which indicate zones susceptible to erosion.

The TRI (Figure 6C) quantifies the degree of terrain heterogeneity by summing the elevation differences between a central cell and its eight neighbors (Brožová et al., 2021). TRI was also calculated using GDAL in QGIS, producing values between 0 to 6.18 m. Lower values (< 1) are associated with flat, well-preserved terrace surfaces, while higher values (> 4) denote abrupt elevation changes often linked to erosion processes or anthropogenic alterations.

The ESD (Figure 6D) was derived in ArcGIS Pro using the *Focal Statistics* tool, applying a 3×3 rectangular neighborhood. This metric captures local variability in elevation. ESD values ranged from 0 to 1.93 m, where values below 0.5 m indicate relatively uniform surfaces, while higher values may reflect microtopographic irregularities due to erosion or human activity.

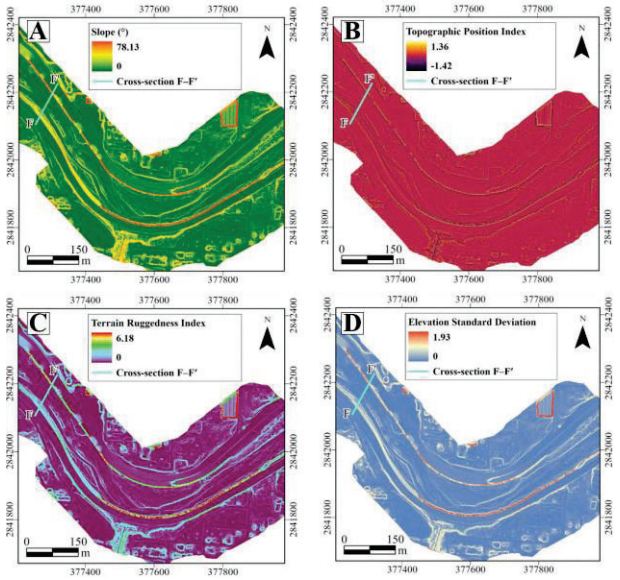

Figure 6. Spatial distribution of the morphometric parameters in the study area: (A) slope, (B) topographic position index, (C) terrain ruggedness index, and (D) elevation standard deviation.

3.3 Geomorphological and Lithological Characterization of the Fluvial Terraces of the Santa Catarina River

In previous studies, such as the one conducted by Martínez Quiroga (2018), three main levels of fluvial terraces were identified and mapped along the Santa Catarina River. However, over time, the landscape has undergone significant natural and anthropogenic changes, associated with extreme hydrometeorological events, erosion and deposition processes, infrastructure development, and urban expansion. Additionally, the limitations of traditional geomorphological interpretation methods used in those earlier studies contributed to reduced spatial precision in terrace delineation.

In this study, the identification and mapping of terraces were updated and refined through the application of high-precision geomatics techniques, including drone-based photogrammetric surveys and the processing of high-density point clouds. This approach enabled the generation of high-resolution DEMs, improving the detection of topographic discontinuities, minor steps, and fluvial surfaces that had not been previously differentiated, such as the newly recognized T0 terrace.

The evolution of the Santa Catarina River's alluvial system is expressed in the presence of at least four distinct terrace levels (T0 to T3), arranged in a stepped pattern along the valley. Each of these units records different phases of sedimentation, flow energy, and degrees of anthropogenic modification, allowing for the reconstruction of the fluvial and sedimentary dynamics of the channel in the context of the MMA (Figure 7).

The characterization was based on the integration of thematic cartography, field observations, lithological analysis, and cross-sectional stratigraphic profiles, which together enabled the identification of the geometry, composition, and relative thickness of each terrace.

3.3.1 The Fluvial Terrace 0 (T0)

T0 corresponds to the most recent and lowest depositional level within the alluvial sequence of the Santa Catarina River. It is located in the current active channel, where surface runoff occurs during ordinary hydrometeorological events.

From a sedimentological perspective, this unit consists of a poorly sorted mixture of sandy silty gravels, featuring small to medium-sized clasts embedded in a silty-sandy matrix. This lithological composition reflects intermittent sediment transport and reworking, typical of an ephemeral stream in an urban environment. Its thickness ranges from 0.5 to 2.5 m.

3.3.2 The Fluvial Terrace 1 (T1)

T1 is characterized by sandy gravels, with clasts predominantly ranging from small to medium size, and exhibiting degrees of roundness from rounded to well-rounded. This terrace shows a notable anthropogenic influence, evidenced by the widespread presence of accumulated solid waste on its surface. In certain areas, surface exposures of the Méndez Formation are also visible. Thicknesses vary between 0.5 and 4 m.

3.3.3 The Fluvial Terrace 2 (T2)

Terrace T2 consists mainly of sandy gravels with small to medium clasts, indicating moderate to high-energy fluvial processes linked to the variable hydrology of the Santa Catarina River. Its discontinuous and fragmented morphology reflects erosion and partial reworking. Thickness ranges from 0.5 to 5 m. In some areas, outcrops of the Méndez Formation reveal stratigraphic links with the regional geological basement.

This contribution has been peer-reviewed. The double-blind peer-review was conducted on the basis of the full paper.
https://doi.org/10.5194/isprs-annals-X-3-W3-2025-77-2026 | © Author(s) 2026. CC BY 4.0 License.

3.3.4 The Fluvial Terrace 3 (T3)

T3 is largely overlain by urban infrastructure, including Dr. Ignacio Morones Prieto Avenue and the Monterrey–Reynosa highway. It is made up of gravelly and sandy materials, with thicknesses ranging between 1 and 7 m. Both the distribution and composition of this unit have been modified by anthropogenic activity, with sectors containing construction debris, road infrastructure, and accumulations of urban solid waste.

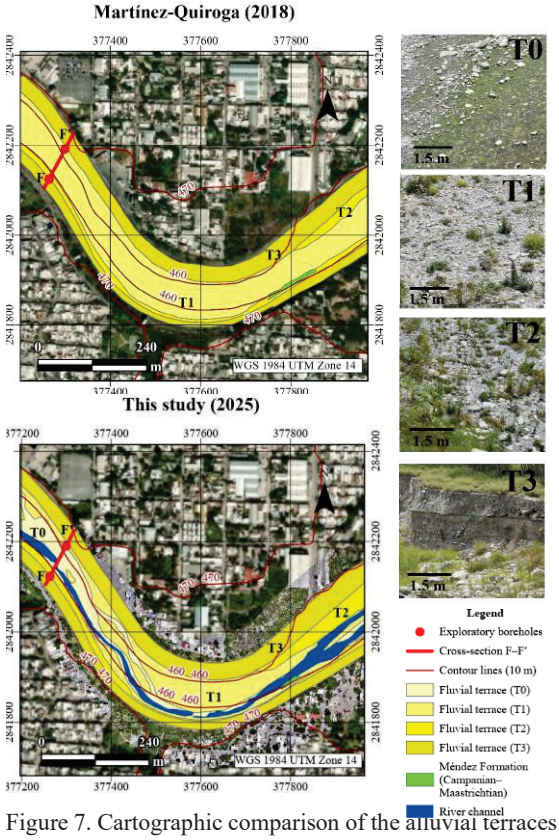

Figure 7. Cartographic comparison of the alluvial terraces of the Santa Catarina River in the urban section of the MMA.

4. Discussion

4.1 Geomorphological Changes Observed

Figure 8 highlights the geomorphological variability along the Santa Catarina River, showing the four levels of alluvial terraces (T0–T3) identified from the point cloud.

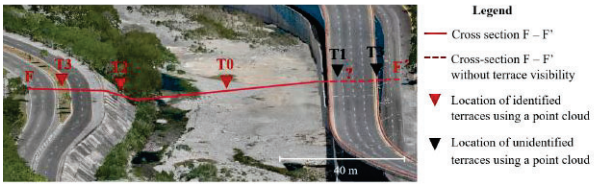

Figure 8. Location of the F–F′ cross-section and identification of fluvial terraces using a point cloud.

Although most terraces were accurately delineated using the 3D model, in areas with limited visibility, marked with dashed lines, it was necessary to complement the interpretation with fieldwork, in situ photographs, and satellite imagery.

Figure 9 reveals geomorphological changes in cross-section F–F′ between 2018 and 2025. The T0 level shows a slight elevation increase in 2025, suggesting sediment accumulation in the channel. T1 presents a slight decrease in elevation, possibly due to surface erosion. In the case of T3, significant alterations are observed as a result of reconstruction works carried out after the river destroyed adjacent roadways during flood events.

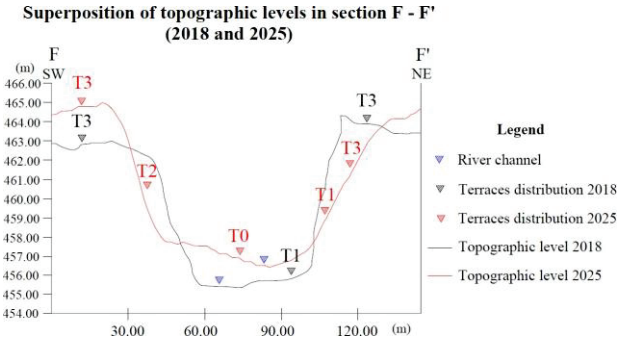

Figure 9. Superposition of topographic profiles and terrace distribution in cross-section F–F′ (2018 and 2025).

These interventions have modified the original morphology of this terrace level. In contrast, T2 and the undisturbed areas of T3 show greater morphological stability.

4.2 Summary of Tropical Cyclones that Have Impacted the Santa Catarina River

This section presents a compilation of tropical cyclones that have impacted Nuevo León from 2018, the year the last study on terraces was completed (Martínez-Quiroga, 2018), to the present (2025).

The "La Huastequita" meteorological station (SMN, 2025), located in Santa Catarina, Nuevo León (latitude: 25.638611° and longitude: -100.455000°), has recorded the main precipitation in the Santa Catarina River.

The SMN (2025) report contains data recorded from 1975 to 2023, so some of these precipitations are related to tropical cyclones recorded by NOAA (2025), and other events were validated by additional sources (SMN, 2013). Furthermore, precipitation data from 2018, the year corresponding to the Martínez-Quiroga (2018) study, were also collected. These data are shown in Table 5.

Date	Precipitation (mm)	Maximum temperature (°C)	Minimum temperature (°C)	Event
07/21/2018	60	38	21	Martínez-Quiroga's study period (2018)
09/26/2018	67.5	33	20	
09/04/2019	220	29	17.5	Tropical Depression Fernand*
07/26/2020	200.8	28	20	Tropical Depression Hanna*
09/18/2020	54	31	13.5	No name

Table 5. Main precipitation and meteorological data within the period 2018 to 2023 were recorded at "La Huastequita" (SMN, 2025).* Source: NOAA (2025).

This contribution has been peer-reviewed. The double-blind peer-review was conducted on the basis of the full paper.
https://doi.org/10.5194/isprs-annals-X-3-W3-2025-77-2026 | © Author(s) 2026. CC BY 4.0 License.

In addition to the information presented by the SMN (2025) and NOAA (2025), there's still one cyclone not yet recorded in those reports, Tropical Storm Alberto. This storm caused maximum precipitation of 600.0 mm according to the El Cerrito station on June 19, 2024, and 282.5 mm reported at the Rodrigo Gómez station on June 20, 2024 (Bravo-Lujano, 2024).

Since the last update on fluvial terrace information by Martínez-Quiroga (2018) to the present, the Santa Catarina River has been impacted by at least three tropical cyclones: Tropical Depression Fernando, Tropical Depression Hanna, and Tropical Storm Alberto. This emphasizes the need for a study regarding the river's fluvial terraces (Figure 10).

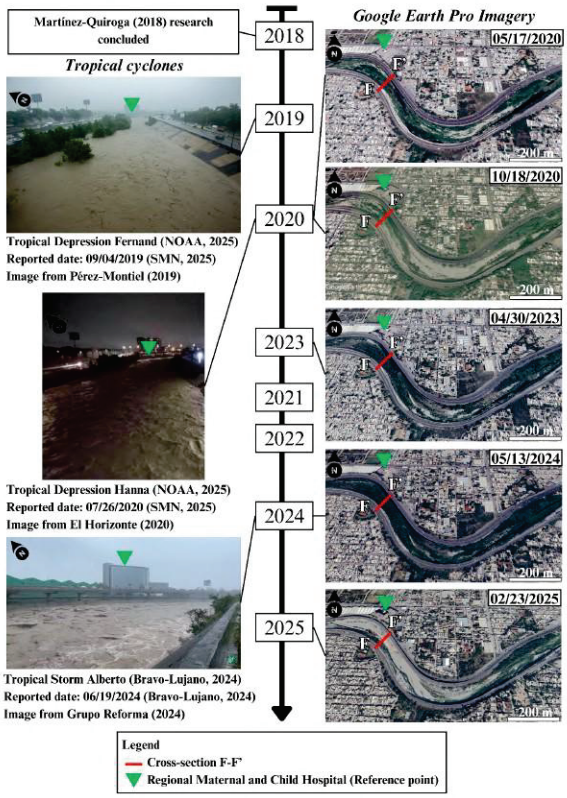

Figure 10. Main tropical cyclones that have occurred since 2018 to the present, and a gallery of satellite images retrieved from Google Earth Pro, where section F-F' is marked. In the images, the Regional Maternal and Child hospital is a reference point.

In Figure 10, the satellite images corresponding to 2020 show an example of a before-and-after scenario following a tropical cyclone. The image marked with the date 05/17/2020 shows the period before Tropical Depression Hanna, where a larger vegetated area can be observed compared to the image after Hanna's passage (10/18/2020), which shows more bare ground and exposes the fluvial terraces.

The same case occurs for 2024 to 2025 (Figure 10); although there is approximately an 8-month difference between the satellite image of 05/13/2024 and 02/23/2025, it can be observed how the rain produced by Tropical Storm Alberto ripped and displaced vegetation, leaving the fluvial terraces exposed.

5. Conclusions

This study demonstrates the effectiveness of integrating UAV-based LiDAR and photogrammetry for the detailed characterization of fluvial terraces in complex urban environments such as the Santa Catarina River.

The post-processing of photogrammetric data and LiDAR point clouds produced high-resolution outputs, including DEMs, orthomosaics (3.08 cm/pixel), and dense RGB-colored 3D point clouds. These products facilitated the detailed geomorphological interpretation of the study area. The classified elevation and intensity values also supported the identification of terrace units, and anthropogenic alterations, proving particularly useful in mapping terrace limits with high spatial precision.

The morphometric analysis based on DEM-derived indices slope, TPI, TRI, and ESD proved effective in identifying and quantifying spatial heterogeneity among terrace surfaces. Low slope, TRI, and ESD values corresponded to well-preserved flat surfaces, while elevated TPI and high TRI values marked areas subjected to erosion and human-induced disturbances, particularly at terrace edges and scarp zones.

By comparing the 2025 data with the 2018 terrace characterization, significant morphological and spatial modifications were identified, revealing both anthropogenic and natural transformations. Socio-environmental factors include the accumulation of solid waste, unauthorized housing within the channel, rubble, wastewater discharges, and civil engineering works. In addition, the recent construction of bridges in the analyzed areas limits UAV-based surveying.

Profile F–F' was selected as a representative example due to its concentration of geomorphological and geological features of interest. This area has been repeatedly affected by extreme hydrometeorological events, which have caused damage to the surrounding road infrastructure, underscoring the active fluvial dynamics within the urban setting of the Santa Catarina River.

Historical cyclone records indicate that F–F' profile has been impacted by at least three events (Tropical Depression Fernando, Tropical Depression Hanna, and Tropical Storm Alberto) which not only altered terrace morphology but also contributed to vegetation displacement and sediment redistribution.

For future UAV-based fluvial terrace studies in urban settings, the following recommendations are proposed: (1) conduct a preliminary survey to identify socio-environmental factors affecting terrace formation and preservation, (2) verify the presence of visual anthropogenic obstructions that may hinder UAV-based data acquisition, and (3) In cases where obstructions are unavoidable, adjust flight planning to modify the angle of view, ensuring comprehensive terrace coverage from alternative perspectives.

The use of UAV-based LiDAR technology enables greater precision and significantly reduces working time in the identification of fluvial terraces. This tool facilitates the detection of morphometric variations and both natural and anthropogenic alterations, providing key information for reducing risks associated with erosion, scouring, and landslide processes.

This study aligns with the United Nations Sustainable Development Goals, goal 6 (Clean water and sanitation), goal 11 (Sustainable cities and communities), goal 13 (Climate action), and goal 15 (Life on land).

This contribution has been peer-reviewed. The double-blind peer-review was conducted on the basis of the full paper.
https://doi.org/10.5194/isprs-annals-X-3-W3-2025-77-2026 | © Author(s) 2026. CC BY 4.0 License.

Acknowledgments

Thanks to the SECIHTI for the financial support to students through their scholarships, for supporting the Graduate Programs and National Researchers involved, and for funding GIRRIO, a Pronaii 2024-35 project.

References

Bravo-Lujano, C., 2024. Informe de la tormenta tropical Alberto. Comisión Nacional del Agua.

Brožová, N., Baggio, T., D'Agostino, V., Bühler, Y., Bebi, P., 2021. Multiscale analysis of surface roughness for the improvement of natural hazard modeling. *Natural Hazards and Earth System Sciences*, 21(11), 3539-3562. https://doi.org/10.5194/nhess-21-3539-2021.

De Reu, J., Bourgeois, J., Bats, M., Zwertvaegher, A., Gelorini, V., De Smedt, P., Chu, W., Antrop, M., De Maeyer, P., Finke, P., Van Meirvenne, Verniers, J., Crombé, P., 2013. Application of the topographic position index to heterogeneous landscapes. *Geomorphology*, 186, 39-49. http://dx.doi.org/10.1016/j.geomorph.2012.12.015

Delchairo, M., Iacobucci, G., Della Seta, M., Gribenski, N., Piacentini, D., Ruscitto, V., Zocchi, M., Troiani, F. 2024. A fluvial record of late Quaternary climate changes and tectonic uplift along the Marche Piedmont Zone of the Apennines: New insights from the Tesino River (Italy). *Geomorphology*, 445, 108971. https://doi.org/10.1016/j.geomorph.2023.108971.

DJI., 2023. Zenmuse L2 User Manual. DJI Enterprise. https://enterprise.dji.com/

El Horizonte, 2020. Tras lluvias de "Hanna", río Santa Catarina llega a su máxima capacidad en Guadalupe. El Horizonte. Recuperado el 11 de junio de 2025, de https://www.elhorizonte.mx/nuevoleon/tras-lluvias-de-hanna-rio-santa-catarina-llega-a-su-maxima-capacidad-en-guadalupe/2898727

Grupo REFORMA, 2024. El Río Santa Catarina se llena tras las lluvias de 'Alberto' (Video). YouTube. https://www.youtube.com/watch?v=lCvfAHiYWZE

Iacobucci, G., Piacentini, D., Troiani, F., 2022. Enhancing the identification and mapping of fluvial terraces combining geomorphological field survey with land-surface quantitative analysis. *Geosciences*, 12, 425. https://doi.org/10.3390/geosciences12110425.

Li, H., Chen, L., Wang, Z., Yu, Z., 2019. Mapping of river terraces with low-cost UAS based structure-from-motion photogrammetry in a complex terrain setting. *Remote sensing*, 11(4), 464. doi:10.3390/rs11040464.

Martínez-Quiroga, G.E., 2018. Caracterización geológica del Río Santa Catarina como base para la elaboración de estudios ambientales de contaminación y abastecimiento de agua potable para el área metropolitana de Monterrey (AMM). MSc. thesis, Universidad Autónoma de Nuevo León.

Martínez-Quiroga, G.E., De León-Gómez, H., Yépez-Rincón, Y.D., López-Saavedra, S., Cardona Benavides, A., Cruz-López, A., 2021. Alluvial terraces and contaminant sources of the Santa Catarina River in the Monterrey Metropolitan Area, México. *Journal of Maps*, 17(2), 247-256. https://doi.org/10.1080/17445647.2021.1898483.

Michalzik, D., 1988. Trias bis teifste Unterkreide der nordöstlichsten Sierra Madre Oriental, Mexiko, Fazielle Entwicklung eines passiven Kontinentalrandes: Darmsatdt, Hesse, Alemania. Universidad Técnica de Darmstadt.

Nagel-Vega, V., 2023. El río Santa Catarina y su histórico vínculo urbano con Monterrey, Nuevo León. *Academia XXII*, 14(28). https://doi.org/10.22201/fa.2007252xp.2023.14.28.87236.

National Oceanic and Atmospheric Administration (NOAA), 2005. Historical hurricane tracks (Interactive map). National Oceanic and Atmospheric Administration. https://coast.noaa.gov/hurricanes/

Niculiță, M., Mărgărint, M.C., Tarolli, P., 2020. Using UAV and LiDAR data for gully geomorphic changes monitoring. In: Tarolli, P., Mudd, S.M. (eds) Remote sensing of geomorphology, vol 23. Developments in Earth Surface Processes. Elsevier, pp. 271-315. doi:10.1016/b978-0-444-64177-9.00010-2.

Pederson, J.L., Anders, M. D., Rittenhour, T.M., Sharp, W.D., Gosse, J.C., Karlstrom, K.E., 2006. Using fill terraces to understand incision rates and evolution of the Colorado River in eastern Grand Canyon, Arizona. *J. Geophys. Res.,* 111, F02003. doi:10.1029/2004JF000201.

Pérez-Montiel, G., 2019. La tormenta tropical "Fernand" entra a Nuevo León, causando intensas lluvias y crecidas en el Río Santa Catarina (Fotografía). Cuartoscuro. https://cuartoscuro.com/fotos/individual/720102/1933

Sánchez-Núñez, J. M., Macías, J.L., Saucedo R., Zamorano, J.J., Movelo, D., Mendoza, M. E., Torres-Hernández, J. R., 2014. Geomorphology, internal structure, and evolution of alluvial fans at Motozintla Chiapas, México. *Geomorphology*, 230, 1-12. https://doi.org/10.1016/j.geomorph.2014.10.003.

Servicio Meteorológico Nacional (SMN), 2010. Reseña del huracán "Alex" del Océano Atlántico. Comisión Nacional del Agua.

Servicio Meteorológico Nacional (SMN), 2025. Normales climatológicas diarias: Estación 19096 "La Huastequita". Comisión Nacional del Agua.

Tlapáková, L., Pánek, T., Horáčková, S., 2021. Holocene fluvial terraces reveal landscape changes in the headwater streams of the Moravskoslezské Beskydy Mountains, Czechia. *Geomorphology*, 377, 107589. https://doi.org/10.1016/j.geomorph.2020.107589.

Yépez, R., Lózano, D., Vela, P., Rivera, L., 2013. Assessing hydrometeorological impacts with terrestrial and aerial Lidar data in Monterrey, México. I*SPRS - International Archives of the Photogrammetry, Remote Sensing and Spatial Information Sciences.* XL-7/W2. 271-276 doi: 10.5194/isprsarchives-XL 7-W2-271-2013.